Title

Endostatin: Yeast Production, Mutants, and Antitumor Effect in Renal Cell Carcinoma

Journal

Cancer Research, 59(1)

ISSN

0008-5472

Authors

Dhanabal, M

Ramchandran, R

Volk, R

et al.

Publication Date

2023-12-12

Peer reviewed

[CANCER RESEARCH 59, 189–197, January 1, 1999]

Endostatin: Yeast Production, Mutants, and Antitumor Effect in Renal Cell Carcinoma[1]

Mohanraj Dhanabal, Ramani Ramchandran, Ruediger Volk, Isaac E. Stillman, Michelle Lombardo, M. L. Iruela-Arispe, Michael Simons, and Vikas P. Sukhatme[2]

Renal [M. D., R. R., V. P. S.] and Cardiology [R. V., M. S.] Divisions, Departments of Medicine and Pathology [M. L., I. E. S., M. L. I-A.], Beth Israel Deaconess Medical Center and Harvard Medical School, Boston, Massachusetts 02215

ABSTRACT

Endostatin is a M_r 20,000 COOH-terminal fragment of collagen XVIII that inhibits the growth of several primary tumors. We report here the cloning and expression of mouse endostatin in both prokaryotic and eukaryotic expression systems. Soluble recombinant protein expressed in yeast (15–20 mg/L) inhibited the proliferation and migration of endothelial cells in response to stimulation by basic fibroblast growth factor. A rabbit polyclonal antibody was raised that showed positive immunoreactivity to the recombinant protein expressed from both systems. Importantly, the biological activity of the mouse recombinant protein could be neutralized by this antiserum in both endothelial proliferation and chorioallantoic membrane assays. Systemic administration of endostatin at 10 mg/kg suppressed the growth of renal cell cancer in a nude mouse model. The inhibition of tumor growth with soluble yeast-produced protein was comparable to that obtained with non-refolded precipitated protein expressed from bacteria. In addition, two closely related COOH-terminal deletion mutants of endostatin were also tested and showed strikingly differing activity. Collectively, these findings demonstrate the expression of a biologically active form of mouse endostatin in yeast, define a role for the molecule in inhibiting endothelial cell migration, extend its antitumor effects to renal cell carcinoma, and provide a formal proof (via the neutralizing antiserum experiments and the mutant data) that endostatin (and not a possible contaminant) acts as an antiangiogenic agent. Finally, the high level expression of mouse endostatin in yeast serves as an endotoxin free, soluble source of protein for fundamental studies on the mechanisms of tumor growth suppression by angiogenesis inhibitors.

INTRODUCTION

Thirty thousand cases of RCC[3] were diagnosed in the United States in 1996 (1). The prognosis for metastatic RCC remains highly unfavorable. Despite advances in radiation therapy and chemotherapy, the long-term survival of treated patients has shown only marginal improvement over the past few decades (1). Because RCC is a highly vascularized tumor, VEGF is likely to play an important role in the formation of tumor-associated angiogenesis. Moreover, the *VHL* gene, lost in >99% of sporadic RCC cases along with alterations of the remaining allele in ≈70% of cases (2), represses VEGF (3–6). In a nude mouse model, introduction of a wild-type *VHL* gene into 786-O cells, a RCC tumor cell line, inhibited tumor growth (7) and angiogenesis. The lack of significant treatment options available for RCC emphasizes the need to focus on the development of novel therapeutic strategies. In this regard, targeting tumor vasculature of solid tumors has recently shown promising results in several animal model systems (8–12).

The growth of solid tumors beyond a few mm^3 depends on the formation of new blood vessels (13). Numerous studies have shown that both primary tumor and metastatic growth are angiogenesis dependent (13–16). A number of angiogenesis inhibitors have been identified. Certain ones, such as platelet factor-4 (17, 18), IFN-α, IFN-inducible protein-10. and PEX (19–21), are not "associated with tumors," whereas two others, angiostatin and endostatin, are "tumor associated" (22, 23). Angiostatin, a potent endogenous inhibitor of angiogenesis generated by tumor-infiltrating macrophages that upregulate matrix metalloelastase (24), inhibits the growth of a wide variety of primary and metastatic tumors (25–29).

Recently, O'Reilly, *et al.* (23) have isolated endostatin, an angiogenesis inhibitor from a murine hemangioendothelioma cell line (EOMA). Circulating levels of a fragment of human endostatin have been detected in patients with chronic renal insufficiency with no detectable tumor (30). The NH_2-terminal sequence of endostatin corresponds to the COOH-terminal portion of collagen XVIII. Endostatin is a specific inhibitor of endothelial proliferation and angiogenesis. Systemic administration of non-refolded precipitated protein expressed in *Escherichia coli* caused growth regression of Lewis lung carcinoma, T241 fibrosarcoma, B16 melanoma, and EOMA (23) cells in a xenograft model. Moreover, no drug resistance was noted in three of the tumor types studied. Surprisingly, repeated cycles of administration with endostatin resulted in tumor dormancy (31).

The results from this study open new avenues for treatment of cancer and provide a promising route for overcoming drug resistance often seen during chemotherapy. However, in all of these investigations, a non-refolded precipitated form of endostatin was administered in the form of a suspension to tumor-bearing animals. In addition, large amounts of protein were required to cause tumor regression and to lead to tumor dormancy. As pointed out by Kerbel (32), an oral drug equivalent of endostatin is needed. Clearly, mechanistic investigations could be undertaken if recombinant protein were available in soluble form. Moreover, initial testing could be done *in vitro* with soluble protein before studying its efficacy under *in vivo* conditions. In the present study, we have obtained the expression of mouse endostatin in the *Pichia pastoris* system. The yeast expression system was selected because of its ability to express heterologous protein in a large scale and to process posttranslational modifications (33, 34). Our studies show for the first time that it is possible to express biologically active mouse endostatin with a yield of 15–20 mg/l of yeast culture. Biological activity was demonstrated *in vitro* by effects on endothelial proliferation and migration (the latter not described previously for endostatin) and in the CAM assay, along with growth inhibition in a RCC tumor xenograft model. For the first time, mutants of the endostatin protein (EM 1 and EM 2) were created, and one mutant (EM 2) showed loss of function in a RCC model.

MATERIALS AND METHODS

Cell Lines. 786-O, a renal clear cell carcinoma line; C-PAE, a bovine pulmonary arterial endothelial cell line; and ECV304, a human endothelial cell line, were all obtained from American Type Culture Collection. The cell lines were maintained in DMEM (786-O and C-PAE) and M199 (ECV304) supplemented with 10% FCS, 100 units/ml of penicillin, 100 μg/ml of strepto-

Received 6/29/98; accepted 10/29/98.

The costs of publication of this article were defrayed in part by the payment of page charges. This article must therefore be hereby marked *advertisement* in accordance with 18 U.S.C. Section 1734 solely to indicate this fact.

[1] This work was supported by seed funds from Beth Israel Deaconess Medical Center and salary support to M. D. via a basic science NIH training grant.

[2] To whom requests for reprints should be addressed, at Beth Israel Deaconess Medical Center, Dana 517, 330 Brookline Avenue, Boston, MA 02215. Phone: (617) 667-2105; Fax: (617) 667-7843; E-mail: vsukhatm@bidmc.harvard.edu.

[3] The abbreviations used are: RCC, renal cell carcinoma; VEGF, vascular endothelial growth factor; CAM, chorioallantoic membrane; bFGF, basic fibroblast growth factor.

mycin, and 2 mM L-glutamine. The cDNA clone for mouse endostatin pBACPak 8 was kindly provided by B. R. Olsen (Department of Cellular Biology, Harvard Medical School, Boston, MA). The prokaryotic expression vector pET17b was purchased from Novagen (Madison, WI). The yeast expression system, *P. pastoris* (pPICZαA). was purchased from Invitrogen (San Diego, CA). Restriction enzymes and Vent DNA polymerase were purchased from New England Biolabs (Beverly, MA).

Cloning and Expression of Mouse Endostatin and Mutants into a Prokaryotic System. The sequence encoding the COOH-terminal portion of mouse collagen XVIII was amplified by PCR using Vent DNA polymerase, and the endostatin pBACPak 8 vector was used as a template. The primers used were 5′-GGC ATA TGC ATA CTC ATC AGG ACT TT-3′ and 5′-AAC TCG AGA TTT GGA GAA AGA GGT-3′.

PCR was carried out for 30 cycles with the following parameters: 94°C denaturation, 60°C for annealing, and 72°C extension, each for 1 min. The amplified DNA fragment (555 bp) was purified using a QIAquick PCR purification kit, digested with *Nde*I and *Xho*I, and ligated into the expression vector pET17bhis (35). Initial transformation was carried out with the HMS 174 host strain. Positive clones were sequenced on both strands. The desired clones were finally transformed into BL21(DE3) for expression. The expression of recombinant protein in the pET system was carried out as described by the manufacturer.

Primers were designed such that 9 and 17 amino acids were deleted from the COOH terminus of endostatin for EM 1 and EM 2, respectively. The amplified DNA fragments (528 bp for EM 1 and 504 bp for EM 2) were purified, digested with *Nde*I and *Not*I, and ligated into a predigested pET28(a) expression vector. The rest of the protocol was carried out as described above. Induction conditions and processing of the bacterial pellet were as described elsewhere (23). The purification of recombinant protein was performed using a Ni-NTA column in the presence of 8 M urea as described in the QIAexpressionist manual. Briefly, the bacterial pellet was solubilized in "equilibration buffer" (8 M urea, 10 mM Tris, and 100 mM sodium phosphate buffer, pH 8.0) for 1 h at room temperature. The suspension was sonicated three to four times and centrifuged at 10,000 $\times$ *g*, and the soluble fraction was loaded on a Ni-NTA column preequilibrated with the above buffer at a flow rate of 10–20 ml/h. The column was washed extensively with equilibration buffer. Bound proteins were eluted by lowering the pH of the buffer (from 8.0 to 6.3, 4.2, and 3.0). For the *in vivo* experiments using endostatin mutants, nonspecific proteins binding to the column were removed by an equilibration buffer wash, followed by 10 mM and 25 mM imidazole washes. Bound proteins were eluted in equilibration buffer containing 0.2 M acetic acid. The purified fractions were analyzed by SDS-PAGE, and the fractions containing purified endostatin (pH 4.2 and 3.0 for wild-type endostatin and equilibration buffer containing 0.2 M acetic acid for endostatin mutants) were pooled and refolded slowly. The final dialysis was carried out against PBS (pH 7.4) at 4°C. During dialysis, the protein precipitated out of solution. It was further concentrated and stored at −70°C in small aliquots. The concentration of protein was determined by the BCA assay (Pierce).

Expression of Mouse Endostatin in *P. pastoris*. The sequence encoding mouse endostatin was further modified by PCR using Vent DNA polymerase. The amplified fragment containing *Eco*RI and *Not*I restriction sites was subcloned into a predigested yeast expression vector. The pPICZαA vector carries an α factor secretion signal sequence with a Zeocin marker for antibiotic selection. Initial transformation was done in the Top 10′ host strain. The resultant clones were screened for insert, and positive clones were sequenced. The plasmid was then linearized with *Sac*I and used for homologous recombination into the yeast host strain GS115. The transformation was carried out by the lithium chloride method as described in the *Pichia* expression manual. Recombinants were selected by plating on YPD plates containing 100 μg/ml of Zeocin. Clones that grew on the YPD/Zeocin plate were tested for expression.

The expression of mouse endostatin in large scale was carried out in 2-liter baffled shaker flasks. The overnight culture (A_{600}, 2–6) was used to inoculate 2-liter flasks, with the addition of 500 ml of buffered glycerol medium. Cells were grown at 250 rpm at 30°C until A_{600}, 16–20 (2 days). Subsequently, cells were centrifuged at 5000 rpm for 10 min, and the yeast were resuspended in 300–400 ml of buffered methanol induction medium. The supernatant containing the secreted recombinant protein was harvested on the second, third, and fourth day after induction. After the final harvest, the cell-free supernatant was processed immediately.

Purification of Mouse Endostatin: Heparin-Agarose Chromatography. The crude supernatant containing recombinant protein was concentrated by ammonium sulfate precipitation (70%). The precipitated protein was dissolved in 10 mM Tris buffer (pH 7.4) containing 150 mM NaCl and dialyzed overnight at 4°C (three changes at 6–8-h intervals). The dialyzed sample was further concentrated by ultrafiltration using an Amicon concentrator (YM 10). A disposable Polyprep column (Bio-Rad) was packed with heparin-agarose resin and equilibrated with 10 mM Tris, 150 mM NaCl, pH 7.4. The concentrated sample was loaded on the column at a flow rate of 20 ml/h using a peristaltic pump. The column was washed with equilibration buffer until the A_{280} was <0.001. Bound proteins were eluted by a step-wise gradient of NaCl (0.3, 0.6, 1, and 2 M NaCl). The peak fractions from 0.6 to 1 M were pooled and dialyzed against PBS (pH 7.4). Protein concentration was measured by the BCA assay (Pierce). The purification process was performed in the cold room (4°C). Recombinant soluble endostatin expressed from the *Pichia* system was used in all of the *in vitro* assays.

Cloning and Expression of His.endostatin into the *Pichia* Expression System. The coding region of the mouse endostatin construct in the pET expression vector is preceded by a His.Tag (10 histidine residues). By DNA-PCR, the coding region including the His.Tag sequence was shuttled into pPICZαA vector. Linearization and recombination into the yeast host strain GS115 were done as described before. The cell-free medium was precipitated with ammonium sulfate (70% saturation). Precipitated proteins were dissolved in 50 mM sodium phosphate buffer (pH 8.0) containing 300 mM NaCl and dialyzed in the same buffer at 4°C after three changes at 6–8-h intervals. A Ni-NTA column was used for purification of the His.endostatin recombinant protein, as described in the QIAexpressionist manual. Bound proteins were eluted with a step-wise gradient of imidazole (10, 25, 50, and 100 mM). The peak fractions from 50 and 100 mM imidazole elutions were pooled and dialyzed against PBS buffer (pH 7.4).

Characterization of Recombinant Yeast Endostatin and Polyclonal Antibody Generation. The purified protein from the yeast expression system was further characterized by NH_2-terminal microsequencing for seven cycles. In addition, a polyclonal antiserum to mouse recombinant endostatin was raised by immunizing a rabbit with 10 μg of purified protein derived from the *Pichia* expression system. Recombinant endostatins expressed from bacteria and yeast systems were separated on 12% SDS-PAGE. The proteins were transferred to polyvinylidene difluoride membrane by semidry transfer (Transblot; Bio-Rad). The primary antiserum was diluted to 1:4000 in 1$\times$ TBS buffer containing 5% nonfat dry milk. Goat anti-rabbit IgG/horseradish peroxidase conjugate was used as a secondary antibody (1:5000). Immunoreactivity was detected by chemiluminescence (Pierce).

Endothelial Proliferation Assay. The antiproliferative effect of endostatin produced in the yeast system was tested using bovine pulmonary artery endothelial cells (C-PAE). The cells were plated in 24-well fibronectin (10 μg/ml)-coated plates at 12,500 cells/well in 0.5 ml of DMEM containing 2% FBS. After a 24-h incubation at 37°C, the medium was replaced with fresh DMEM and 2% FBS containing 3 ng/ml of bFGF (R & D systems) with or without recombinant mouse endostatin. The cells were pulsed with 1 μCi of [^{3}H]thymidine for 24 h. Medium was aspirated, cells were washed three times with PBS, and then solubilized by addition of 1.5 N NaOH (100 μl/well) and incubated at 37°C for 30 min. Cell-associated radioactivity was determined with a liquid scintillation counter.

Migration Assay. To determine the ability of recombinant endostatin to block migration of ECV304 cells toward bFGF, a migration assay was performed using 12-well Boyden chemotaxis chambers (Neuro Probe, Inc.) with a polycarbonate membrane (25 $\times$ 80-mm, PVD free, 8-μm pores; Poretics Corp., Livermore, CA). The nonspecific binding of growth factor to the chambers was prevented by coating the chambers with a solution containing 0.5% gelatin, 1 mM $CaCl_2$, and 150 mM NaCl at 37°C overnight. ECV304 cells were grown in 10% FBS containing 5 ng/ml 1,1′-dioctadecyl-3,3,3′,3′-tetramethylindocarbocyanine perchlorate (DiIC18; Molecular Probes, Eugene, OR) overnight and washed with PBS containing 0.5% BSA. After trypsinization, the cells were counted using Coulter Counter Z1 (Luton, United Kingdom) and diluted to 300,000 cells/ml in Medium 199 containing 0.5% FBS. The lower chamber was filled with Medium 199 containing 25 ng/ml bFGF. The upper chamber was seeded with 15,000 cells/well with different concentrations of

recombinant endostatin. Cells were allowed to migrate for 4 h at 37°C. At that time, the cells on the upper surface of the membrane were removed with a cell scraper, and the (migrated) cells on the lower surface were fixed in 3% formaldehyde and washed in PBS. Images of the fixed membrane were obtained using fluorescence microscopy at 550 nM with a digital camera, and the number of cells on each membrane was determined using the OPTIMAS (version 6.0) software.

CAM Assay. The ability of mouse endostatin to block bFGF-induced angiogenesis *in vivo* was tested using the CAM assay. Fertilized white Leghorn chicken eggs (SPAFAS, Inc., Norwich, CT) were opened on 100-mm^2 Petri dishes and allowed to grow until day 11 in a humidified incubator at 38°C. Pellets containing Vitrogen (Collagen Biomaterials, Palo Alto, CA) at a concentration of 0.73 mg/ml and supplemented with: (*a*) vehicle alone; (*b*) VEGF (250 ng/pellet); (*c*) VEGF and endostatin (20 to 0.5 μg/pellet); (*d*) bFGF (50 ng/pellet); and (*e*) bFGF and endostatin (20 to 0.5 μg/pellet) were allowed to polymerize at 37°C for 2 h. The pellets were placed on a nylon mesh and oriented on the periphery of the CAM. Embryos were returned to the incubator for 24 h. Invasion of new capillaries on the collagen mesh was assessed by injection of FITC-dextran into the circulation of the chicken embryo. At the end of the experiment, the meshes were dissected, and evaluation of vascular density was done using the program NIH Image 1.59, as described previously (36). Assays were performed in triplicate, and four independent experiments were conducted.

Neutralization of the Inhibitory Effect of Endostatin. The specificity of the inhibitory effect of endostatin was demonstrated by neutralization studies using endothelial proliferation and CAM assays. Briefly, in the endothelial proliferation assay, the endostatin was preincubated with polyclonal antiserum or purified antibody (IgG) and then added to the C-PAE cells. Preimmune serum was used as negative control. In addition, purified IgG and endostatin antibody alone were also used as a control. The cells were then pulsed with [^{3}H]thymidine for 24 h, and cell-associated radioactivity was measured as described before. For the CAM assay, endostatin (10 μg) and antiserum (50 μg) were preincubated overnight end-over-end at 4°C prior to preparation of the pellets. Controls for these experiments included IgG alone and preimmune serum alone. Evaluation of the angiogenic response was determined as indicated above.

RCC Tumor Model. Male nude mice, 6–8 weeks of age, received injections s.c. in the right flank with 2 million 786-O cells in a 100-μl volume. Tumors appeared ~2 weeks after implantation. Tumor size was measured using calipers, and tumor volume was calculated using a standard formula (22). The tumor volume ranged from 350 to 400 mm^3. The animals were randomized, and each group had five mice with comparable tumor size within and among the groups. Treatment was started with recombinant endostatin (bacterial or yeast versions), with each mouse receiving 10 mg/kg body weight of recombinant protein daily, administered for a period of 10 days via i.p. injection. Control animals received PBS each day. Tumor size in all groups was measured on alternate days, and tumor volume was calculated. The treatment was terminated on day 10, and animals were sacrificed; tumors from each mouse were removed and fixed in 10% buffered formalin.

For the mutant study, each mouse received 20 mg/kg body weight of the protein daily for 2 weeks i.p. The initial tumor volume was 150–200 mm^3. Wild-type endostatin, also produced in the pET28(a) vector, was given at 20 mg/kg body weight for the experiment as a positive control, and PBS was given as a negative control.

RESULTS

Mouse Endostatin and Its Mutants Can Be Expressed and Purified from a Bacterial Expression System. The gene encoding mouse endostatin was amplified from the pBACPak8 plasmid and expressed initially in the pET expression system. A Ni-NTA agarose column was used to purify the recombinant protein (Fig. 1*A*). Protein present in inclusion bodies was solubilized in 8 M urea and purified under denaturing conditions as described by O'Reilly *et al.* (23). SDS-PAGE analysis showed a discrete band at M_r 22,000–24,000 under nonreducing conditions (Fig. 1*B*). In addition, higher molecular complexes were also observed, which upon reduction resulted in a discrete band at M_r 22,000–24,000. The peaks at different pH elutions

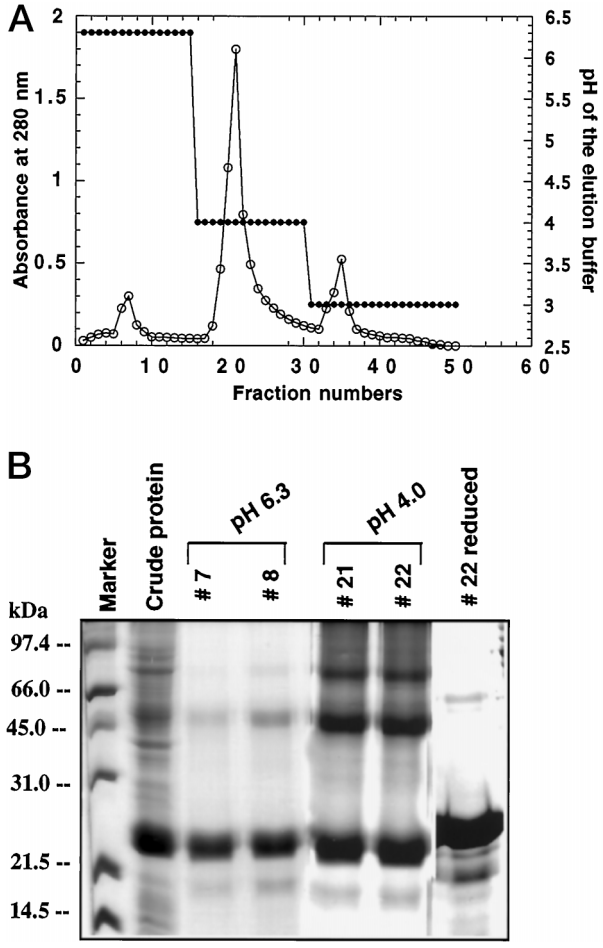

Fig. 1. *A*, purification of recombinant mouse endostatin using a Ni-NTA column, under denaturing conditions. The solubilized protein containing 8 M urea was loaded on a Ni-NTA column, and the bound protein eluted by decreasing the pH of the elution buffer. ●, pH of the elution buffer; ○, absorbance at 280 nm. *B*, protein analysis by SDS-PAGE. *Left*, low molecular weight protein standards (in thousands). Ten μl of selected fractions from each elution point were analyzed. In addition to the expected M_r 22,000–24,000 protein, considerable amounts of higher molecular weight complexes corresponding to M_r 46,000 and M_r 69,000 were also seen. With DTT, all of the higher molecular weight complexes converted to a monomeric subunit corresponding to M_r 22,000–24,000.

(pH 4.2 and 3.0) were pooled and dialyzed against decreasing concentrations of urea, and final dialysis was performed in PBS buffer (pH 7.4), at which time most of the proteins precipitated out of solution. Because non-refolded precipitated protein expressed from a similar system had shown biological activity *in vivo*, we followed the exact procedure used for "protein refolding" [as described by O'Reilly *et al.* (23)]. The precipitated protein was used in suspension form for *in vivo* experiments only, with the concentration of protein measured by the BCA method (solubilized in urea with a suitable blank) and stored at −70°C in small aliquots. Because mouse and human endostatin are strikingly conserved at the COOH terminus, we made two small deletions, reasoning that larger deletions may destroy activity. EM 1, a M_r 19,000 protein, was generated with an 9-amino acid deletion from the COOH terminus, leaving all of the four cysteine residues intact. EM 2 was an additional 8-amino acid deletion that omitted the most COOH-terminal cysteine.

Purification and Characterization of Yeast-derived Soluble Endostatin. *P. pastoris*, a methanotropic yeast strain, has many advantages of a higher eukaryotic expression system: (*a*) the presence of α factor signal sequence facilitates secretion of the expressed protein into the medium; (*b*) the yeast strain (GS115) secretes only very low levels of endogenous host protein, which further simplifies the puri-

fication process; (*c*) endotoxin contamination is not an issue; and (*d*) glycosylation can occur. The pPICZαA vector was selected for expression of mouse endostatin. Initial screening was used to identify yeast clones with high levels of expression. Endostatin was expressed as a soluble protein (M_r 20,000), with a peak level of expression noted on the second day after induction.

A heparin-agarose column was used for purification, based on data of O'Reilly *et al.* (23). Fig. 2 shows the elution profile and SDS-PAGE analysis of purified protein. Two distinct peaks were obtained with increasing concentration of NaCl (Fig. 2*A*). The first peak at 0.3 M NaCl was small when compared with the major peak at 0.6 M NaCl. Most of the endostatin protein bound to the column as shown by the lack of the protein in the flow-through fraction (Fig. 2*B*). The recombinant protein bound tightly, and washing with the low-salt Tris buffer removed other yeast-derived proteins. Protein eluted from the 0.3 M NaCl fraction had a trace amount of endostatin but was contaminated with other host-derived, high molecular weight protein. The purified protein migrated at M_r 20,000, which upon reduction migrated at M_r 22,000. The protein fractions eluted at 0.6 M and 1 M NaCl were pooled, concentrated, and dialyzed against PBS (pH 7.4). The purified protein was further separated by FPLC using a Superose 12 size separation column. The elution profile from this column showed a single peak (data not shown). SDS-PAGE analysis showed the presence of single discrete band corresponding to endostatin (data not shown). The level of expression was estimated to be in the range of 15–20 mg/l culture.

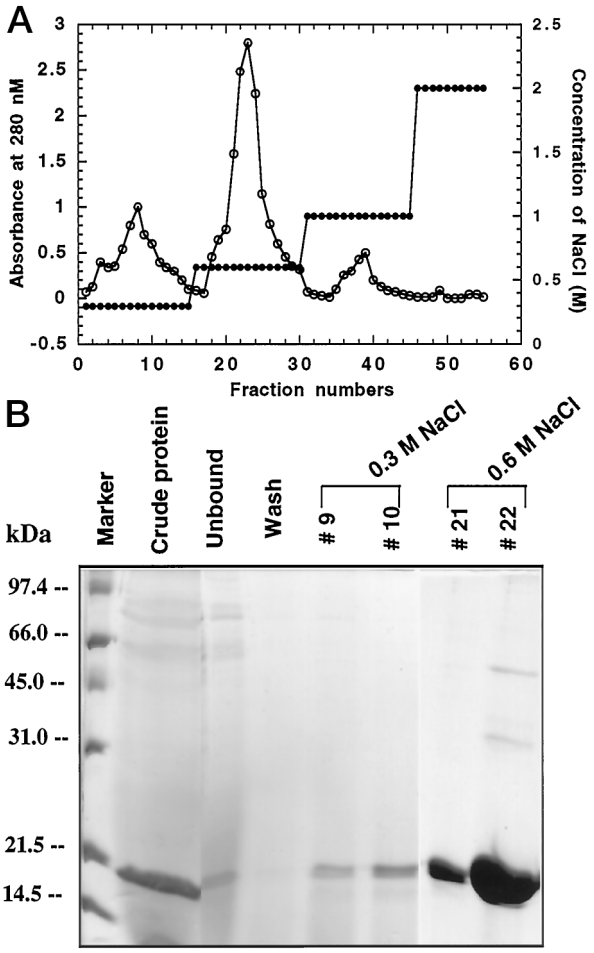

Fig. 2. *A*, purification of soluble mouse endostatin expressed in yeast using a heparin-agarose column. Concentrated supernatant from a one liter culture was loaded in batches. Step-wise gradient of NaCl from 0.3, 0.6, 1, and 2 M was used to elute bound endostatin from the column. Two ml of eluted fractions were collected per tube. ●, concentration of NaCl; ○, absorbance at 280 nm. *B*, electrophoretic analysis of purified recombinant soluble mouse endostatin from heparin-agarose column by 12% SDS-PAGE. *Left*, low molecular weight standards (in thousands). The purified protein migrated as a single band corresponding to M_r 20,000. A 10-μl aliquot of selected fractions was used for analysis of purity of the eluted protein.

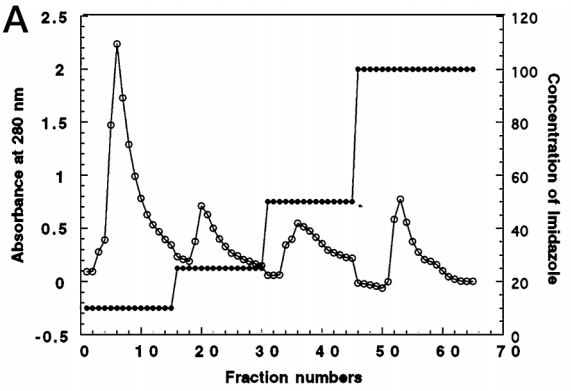

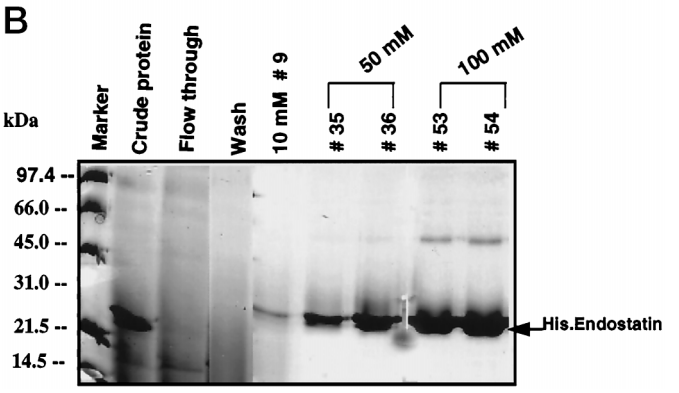

Fig. 3. *A*, purification of soluble His.endostatin expressed in yeast using a Ni-NTA column. Elution profile from the Ni-NTA column. A step-wise gradient of imidazole (10, 25, 50, and 100 mM) was used to elute the bound proteins from the column. ●, concentration of imidazole; ○, absorbance at 280 nm. *B*, 12% nonreducing SDS-PAGE of selected fractions. *Left*, low molecular weight standards (in thousands). Purified recombinant His.endostatin migrated as a single band corresponding to M_r 22,000–24,000 in 50 mM imidazole, whereas 100 mM elution showed a trace amount of higher molecular weight complexes corresponding to M_r 44,000–46,000.

To further characterize the recombinant protein, NH_2-terminal microsequencing was carried out at the Harvard microsequencing facility. It showed that the yeast α factor signal peptide was processed and cleaved at alanine. The first seven residues (EFHTHQD) of the purified protein after signal peptide cleavage matched exactly the published sequence of endostatin protein (data not shown), with the first two residues (EF) derived from linker sequence.

Generation of a Soluble His-tagged Endostatin (His.endostatin) in Yeast. The elution profile of His.endostatin from the Ni-NTA column showed that the recombinant protein bound tightly (Fig. 3). The yeast-derived host proteins in the culture supernatant did not bind to the column and were removed during the wash. Bound proteins were eluted by a stepwise gradient of imidazole (Fig. 3*A*). The nonspecifically bound, host-derived proteins eluted with the addition of 10 mM imidazole. At 25 mM imidazole, a small fraction of the recombinant protein was eluted, along with proteins of higher molecular weight. Final elution with 50 and 100 mM imidazole showed a distinct peak. SDS-PAGE analysis (Fig. 3*B*) of the eluted proteins showed that the flow-through fraction did not contain any endostatin, indicating that most of the protein bound to the column. Increasing the concentration of imidazole to 10 and 25 mM resulted in the elution of nonspecific protein. A protein with M_r 22,000 was seen at 100 mM,

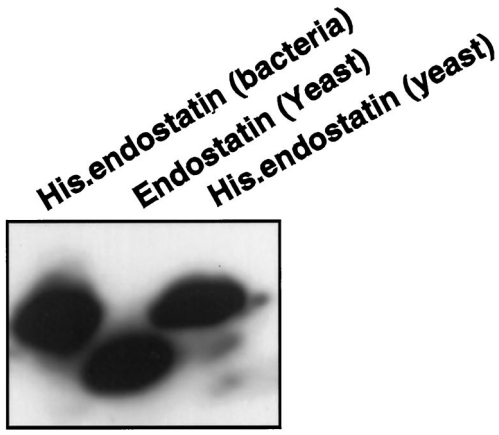

Fig. 4. Western blot analysis of recombinant mouse endostatin expressed from bacteria and yeast. The purified protein was separated by 12% SDS-PAGE and immunoblotted with antiserum raised to a yeast soluble endostatin. The primary antiserum was used at 1:4000 dilution; secondary antibody was anti-rabbit IgG conjugated to horseradish peroxidase (1:5000). Immunoreactivity was detected by chemiluminescence.

along with a smaller amount of protein corresponding to M_r 44,000–46,000. The concentration of purified protein was determined by the BCA method. The level of expression was estimated at 15 mg/l culture.

Western Blot Analysis. A polyclonal antibody was raised against purified mouse endostatin derived from the yeast expression system. The purified endostatin expressed from the bacterial and yeast expression systems were run under reducing and nonreducing conditions. Fig. 4 shows immunoreactive bands corresponding to endostatin. The size of the protein estimated from the Western blot ranges from M_r 22,000–24,000. In addition, the recombinant His.endostatin from yeast and bacteria was probed with a Penta His.monoclonal antibody (Qiagen, Santa Clarita, CA). The monoclonal antibody showed positive response only with the His.endostatin, whereas native endostatin did not show any immunoreactivity (data not shown). This data confirmed the presence of the His.Tag in the recombinant protein. The antiserum did not show any cross-reactivity to human or mouse angiostatin, demonstrating some degree of immunoreactivity specific to endostatin (data not shown). Immunoreactivity of the polyclonal antibody was also observed with EM 1 and EM 2 proteins (data not shown).

Yeast-produced Endostatin Has Antiproliferative Effects on Endothelial Cells. The antiproliferative effect of endostatin produced in the yeast system was tested using C-PAE cells. We initially experimented with different endothelial cell types and tested various parameters [time of "starvation," serum concentration, concentration and type of mitogenic stimulus (VEGF *versus* bFGF)]. C-PAE cells gave the most reproducible response. A dose-dependent inhibition of bFGF-induced proliferation was seen (Fig. 5*A*). The inhibition range (30–94% of control) was seen with increasing concentrations of endostatin (0.1–10 μg/ml), with an ED_{50} in the range of 600–700 ng/ml. A similar inhibitory effect on C-PAE cells was seen when His.endostatin from yeast was tested in the above assay (Fig. 5*A*). The recombinant protein did not inhibit the proliferation of the RCC cells (786-O and A498) at concentrations ranging from 0.5 to 10 μg/ml (Fig. 5*B*), nor did it have an effect on IMR90 and NIH3T3 fibroblasts (data not shown).

Yeast-produced Endostatin Blocks Endothelial Cell Migration. Because C-PAE cells do not migrate in response to bFGF and VEGF, ECV304 cells were used with different concentrations of endostatin using bFGF as a stimulus. Addition of endostatin resulted in a dose-dependent inhibition of migration (Fig. 6). At a concentration <1 μg/ml, marginal inhibition of migration was noted, whereas at 10 μg/ml, 60% inhibition of endothelial cell migration was observed. These studies are the first to show the effect of endostatin on cell migration. The action of endostatin on migration of two non-endothelial cell lines was also assessed. No effect was seen on inner medullary collecting duct renal cells, and some effect (15% at 5 μg/ml and 50% at 20 μg/ml) was noted in the IC-21 macrophage precursor cell line (data not shown), suggesting that at high concentration, endostatin may block cell migration in some cell types.

Yeast-produced Endostatin Has a Dramatic Effect in the CAM Assay. Endostatin was able to suppress the angiogenic response mediated by both bFGF and VEGF (Fig. 7). The inhibition was dose dependent. Blocking of the VEGF response was somewhat more effective (47%) than the suppression of the bFGF response (39%), both at 20 μg/mesh.

Neutralization of Endostatin Activity. The ability of our polyclonal antiserum to neutralize the biological activity of endostatin was tested in both endothelial proliferation and CAM assays. Fig. 8 demonstrates that the inhibitory effect of endostatin can be suppressed by incubation with specific antiserum. Anti-endostatin antiserum blocked the suppressive effect by 95% (data not shown). The preim-

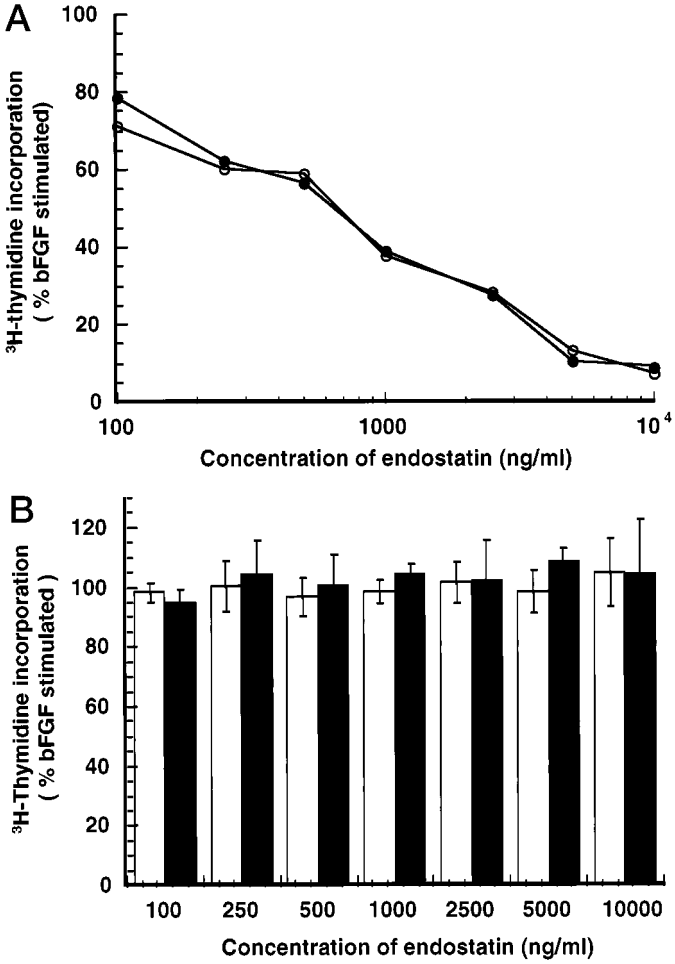

Fig. 5. *A*, endothelial cell proliferation assay. The purified mouse endostatin expressed from yeast was tested for its ability to inhibit [*methyl*-^{3}H]thymidine incorporation in C-PAE cells. bFGF at 3 ng/ml was used as a stimulus, along with 2% serum. Each value is a mean of triplicate cultures from a representative experiment; *bars*, SD. DNA synthesis in the control culture was considered as 100%. The experiment was repeated five times under identical conditions with similar results for yeast-derived soluble endostatin (○) and yeast-derived soluble His.endostatin (●). *B*, effect of endostatin on non-endothelial cells. Open bars refer to 786−0 cells, and shaded bars refer to A498. Both are RCC lines stimulated with bFGF (3 ng/ml) in 2% serum.

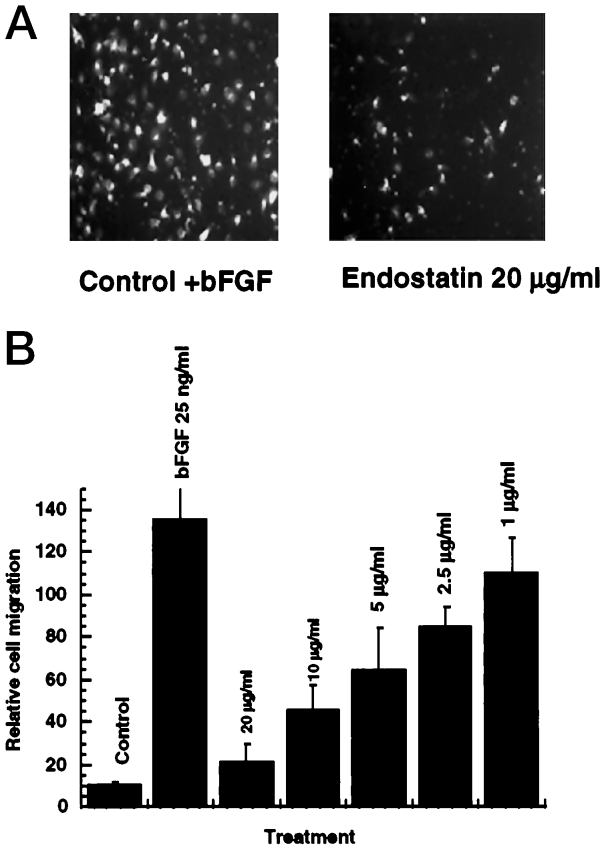

Fig. 6. *A*, inhibition of endothelial cell (ECV 304) migration by soluble mouse endostatin using bFGF (25 ng/ml) as a stimulus. Endothelial cells were allowed to migrate for 4 h at 37°C. The number of cells migrating in the presence or absence of endostatin was calculated using the OPTIMAS 6.0 version software. A representative picture of migrated endothelial cells in control (+*bFGF*, no endostatin) and endostatin (20 μg/ml) with bFGF is shown. *B*, inhibition of endothelial cell migration with different concentrations of endostatin. Each treatment was done in duplicate. In each well, the number of cells migrated was counted in three different areas, and the average obtained. Each value is a mean from representative experiments; *bars*, SD.

mune serum and endostatin antibody alone did not have stimulatory effect nor did normal rabbit IgG.

Inhibition of Primary 786-O RCC Tumors in Nude Mouse Model. Recombinant endostatin was administered daily at 10 mg/kg/day when the tumor size was ~350–400 mm^3. On the fifth day after treatment, there was a difference between control (963 mm^3) and treated (Endo yeast, 405 mm^3; endo bacteria, 442 mm^3; and His.endo, 462 mm^3) groups. A 2.5-fold decrease in tumor volume was observed on the fifth day after treatment between control and treated groups (Fig. 9, *A* and *B*). The growth of the tumor was suppressed in all of the treatment groups: a slower growth rate was seen compared with the control group. Bacterial (His.Tag) or yeast-derived (with or without His.Tag) endostatin at a dose of 10 mg/kg all worked equally well. On the tenth day after treatment, the tumor volume in the control animals was 1490 mm^3, whereas in the treated group, it was in the range of 480–570 mm^3 ($P < 0.005$). Endostatin administration did not inhibit tumor growth completely: the growth of the tumors slowed, with a marginal increase in volume during the treatment period.

Two Closely Related COOH Terminus Endostatin Mutants Generated in *E. coli* Show Markedly Differing *in Vivo* Activity in RCC. A second set of experiments with endostatin and mutants EM 1 and EM 2 at a dosage of 20 mg/kg body weight were conducted in a RCC model, as a first step in exploring structure-function relationships. Nine days after treatment, the difference between groups was apparent (Fig. 9*C*). On the eleventh day after treatment, the tumor volume in the control group (397 mm^3) was approximately twice that of the two treated groups: endostatin (182 mm^3) or EM 1 (259 mm^3). However, on the same day, the tumor volume of the EM 2-treated group (389 mm^3) was similar to that of the control group (397 mm^3). Significance was at the 90% confidence level between the EM 2 and endostatin groups and 95% confidence level between endostatin and control groups. Dropping the value of the largest and smallest tumors on day 11 in each group increased the confidence level to 95% between EM 2 and EM 1 and between EM 2 and endostatin. Therefore, EM 1 protein retained the native biological activity of endostatin, whereas EM 2 with an additional 8 amino acids deleted did not. Also, of note, two of the five mice in the endostatin group and one of five in the EM 1 group had no detectable tumor at the end of the treatment period.

DISCUSSION

In the present study, we have shown that biologically active mouse endostatin can be expressed at high levels in the *P. pastoris* yeast expression system. This system has all of the advantages of an eukaryotic expression system and generally gives higher expression levels (34, 37). It has the added advantage of inducible expression, leading to 10–100-fold higher heterologous protein expression levels compared with other eukaryotic systems (baculovirus or mammalian) with values as high as 1–10 g/l culture when optimized in a fermenter (38). Moreover, endostatin expressed from the *Pichia* system was secreted into the medium with a molecular weight of M_r 20,000, in agreement with the size obtained from other sources (23), and was biologically active *in vitro* and *in vivo*.

The recombinant protein bound to a heparin-agarose column and was eluted at 0.6–1 M NaCl concentration. These data suggested that the yeast expressed protein was folded properly, because the ED_{50} was comparable with that obtained with baculovirus-expressed protein (ED_{50} ≈600–700 ng/ml; Ref. 23). Also, endostatin at high doses (>100 μg/ml) did not inhibit the growth of the 786-O cell line. Microsequence analysis confirmed the processing of the signal peptide, and the NH_2-terminal amino acids matched with published sequence. In the CAM assay, endostatin at 20 μg/disc inhibited angiogenesis induced by bFGF. Similar findings have also been reported as data not shown using baculovirus-expressed endostatin (23). The effect of endostatin on the CAM assay showed more potency on a molar basis than the inhibitors thrombospondin-1 (36), fumagillin (AGM 1470), or antibodies against the integrin $\alpha_v\beta_3$.[4] Our studies on endothelial cell migration provide an additional mechanism of action for endostatin and a new *in vitro* assay for its efficacy.

In vivo, both *E. coli*-derived protein and yeast-produced soluble protein gave comparable inhibitory profiles. Moreover, the presence of a His.Tag sequence in the yeast-derived protein did not affect biological activity. O'Reilly *et al.* (23) reported that endostatin at 10 mg/kg inhibited tumor growth by 97%. In our first study, we failed to see such a dramatic response. Although there was significant difference in tumor volume between control and treated mice, the tumors in the treated group continued to grow slowly. On the tenth day after treatment, when administration of endostatin was stopped, the tumor grew rapidly, and within a week, the average size of the tumors was comparable with controls (data not shown). Subsequently, we tested the effects of endostatin (and its mutants) on tumors ranging from 150 to 200 mm^3 and also increased the endostatin dosage to 20 mg/kg body weight. Three of 10 mice in the combined endostatin and EM 1 groups showed regression. Possible explanations for our differences with O'Reilly *et al.* (23) include: (*a*) protein was given i.p. (our data)

[4] M. L. Iruela-Arispe, unpublished observations.

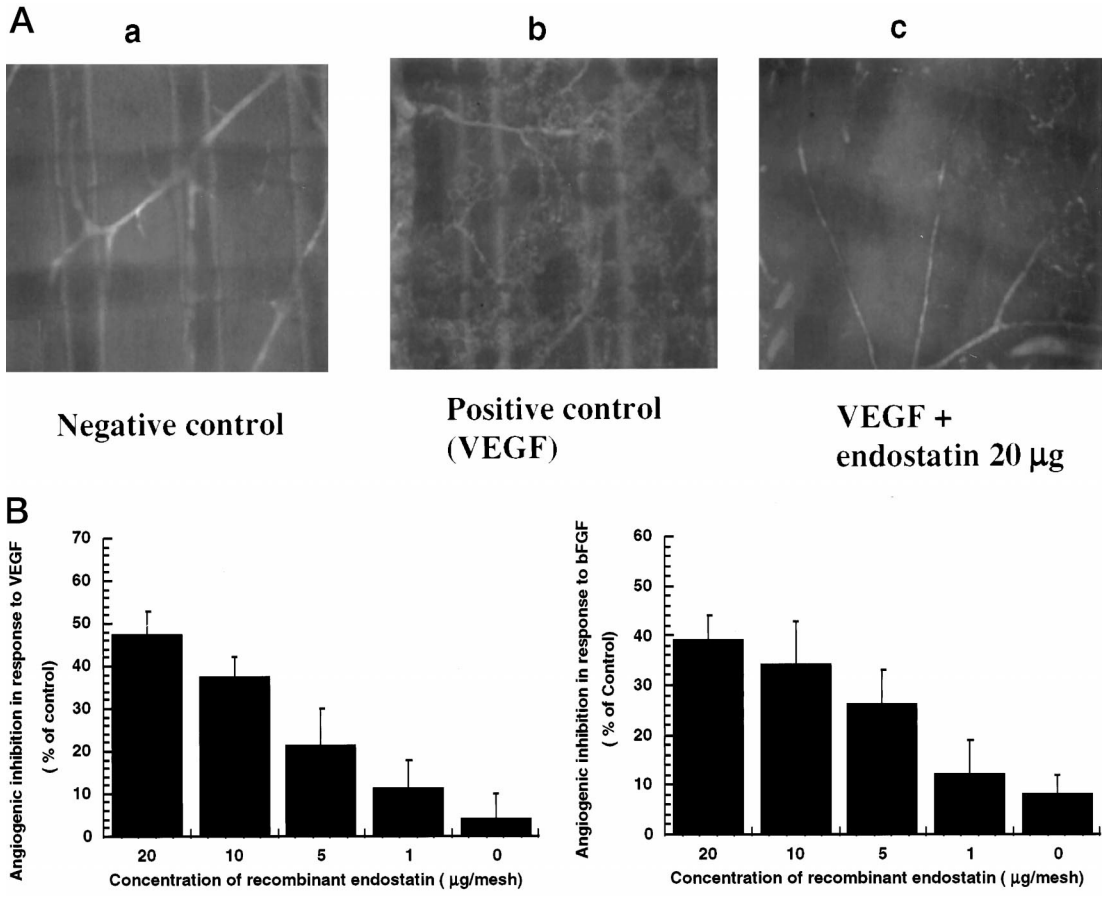

Fig. 7. *A*, inhibition of angiogenic response mediated by VEGF (250 ng/pellet) in the presence of endostatin. Fifty μl of purified recombinant endostatin (20 μg) were added to an aliquot of Vitrogen, and the mixture was placed on a nylon mesh. After polymerization, meshes were placed on the chick embryo and incubated at 37°C for 24 h. New vessel growth was assessed after injecting the vessel with FITC-dextran. *a*, negative control; *b*, positive control (VEGF); *c*, endostatin plus VEGF. *B*, inhibition of VEGF (*left*) and bFGF (*right) mediated angiogenic response by endostatin in the CAM assay. Different concentrations of endostatin were added on the nylon mesh, and vessel growth was determined as described before. All of the counts were normalized to the negative control. Bars, SD.*

versus s.c. (23); and (*b*) the response of this tumor (RCC) to antiangiogenic treatment may be different from that of other tumor types (23) in that RCC may secrete either higher levels or different types of angiogenic proteins. To obtain greater efficacy, it may be possible in the future to tailor the treatment option (*e.g.*, type of antiangiogenic therapy), depending upon the angiogenic stimulator secreted by the tumor. Additionally, other modalities, such as chemotherapy and radiation (not efficacious as single agents in RCC), or biologicals

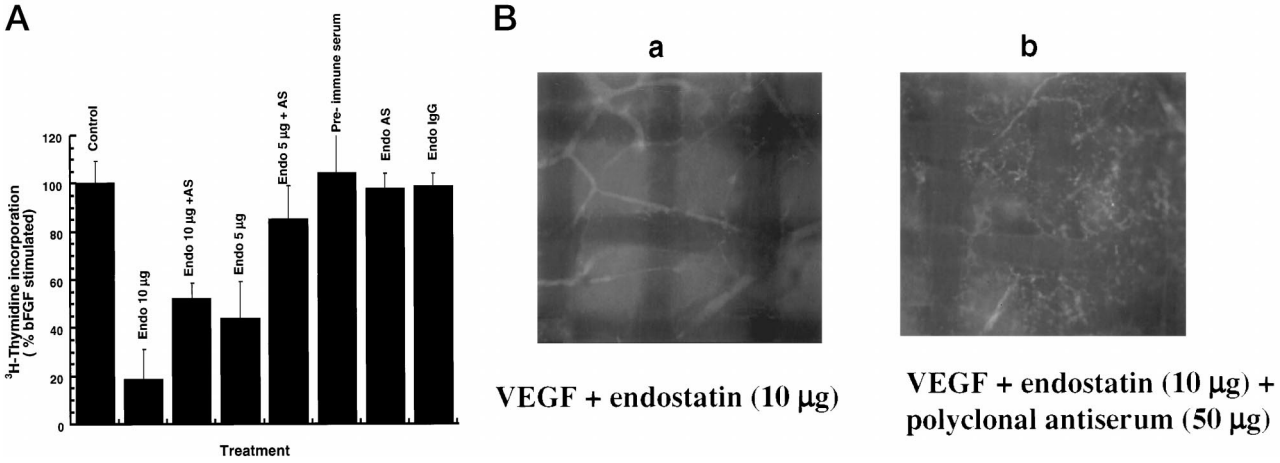

Fig. 8. *A*, neutralization of the inhibitory effect of mouse endostatin by polyclonal antiserum in the endothelial proliferation assay. A 24-well, fibronectin-coated plate was seeded with C-PAE cells at 12,500 cells/well. Recombinant endostatin (10 and 5 μg/ml) was mixed with excess of polyclonal antiserum to endostatin or preimmune or control IgG for 1 h at room temperature. The mixture was then added to C-PAE cells in the presence of 3 μg/ml bFGF. DNA synthesis was measured by adding 1 μci/well [^{3}H]thymidine. Each value is a mean from triplicate culture; *bars*, SD. *B*, neutralization of endostatin inhibitory activity by polyclonal antiserum. The angiogenic response induced by VEGF (250 ng/pellet) was inhibited by preincubating recombinant protein with polyclonal antiserum against endostatin. The incubation with antiserum was done at 4°C overnight, and the mixture was added to a nylon mesh containing Vitrogen. *a*, VEGF and endostatin (10 μg/pellet); *b*, endostatin (10 μg/pellet) plus polyclonal antiserum plus VEGF.

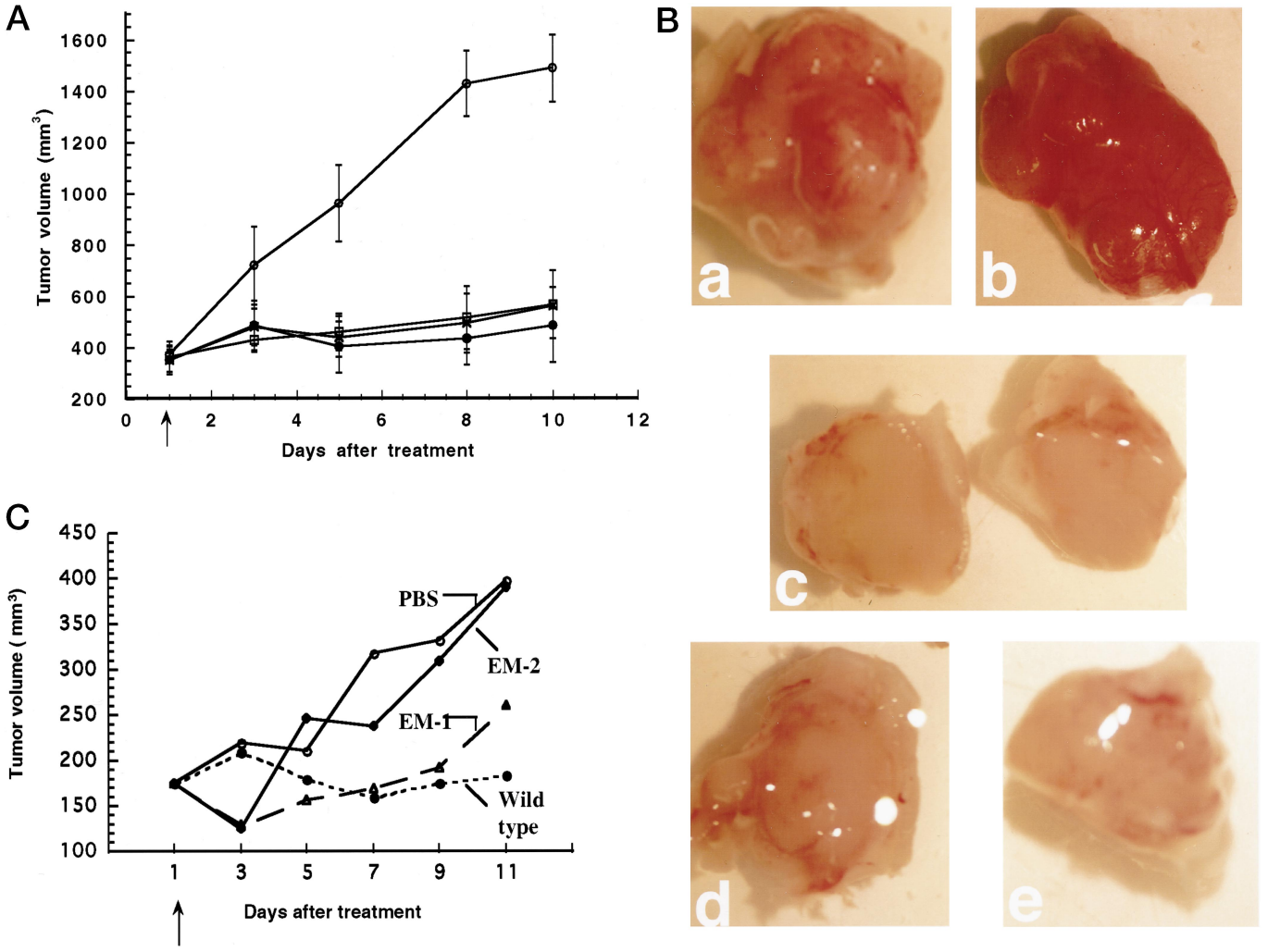

Fig. 9. *A*, inhibition of 786-O tumor growth by systemic treatment with recombinant endostatin. Athymic nude mice carrying 786-O tumor cells were treated with recombinant endostatin from bacteria and yeast when the tumor volume was ~350–400 mm^3. i.p. injection of endostatin was given at 10 mg/kg/day, starting on day 1 (*arrow*). Each time point represents the average of five mice in each group; *bars*, SE. ○, control PBS; ●, endostatin from yeast; ×, His.endostatin from yeast; □, His.endostatin from bacteria. *B*, at the end of the treatment period, tumors from control and treated groups were examined grossly under a dissecting microscope. Tumors from the control group were in general larger and more highly vascularized: *a* and *b*, control; *c*, endostatin from yeast; *d*, His.endostatin from bacteria; and *e*, His.endostatin from yeast. *C*, effects of endostatin mutants on athymic nude mice 786-O tumors. Treatment with recombinant endostatin was begun when the tumor volume was ~150–200 mm^3. i.p. injection of endostatin was given at 20 mg/kg on a daily basis. Each time point represents the average of five mice in each group. ○, control PBS; ●, wild-type His.endostatin from bacteria; Δ, EM 1 from bacteria; ♦, EM 2 from bacteria. Note that EM 1 and EM 2 contain NH_2 terminus His tags.

(IL-2, IFN) could be combined with endostatin to provide synergism, as has been demonstrated recently for angiostatin (39).

Our data with neutralizing antibody and the two mutant endostatin proteins (with markedly differing efficacy) provide further evidence that endostatin and not a possible contaminant is the active molecule giving an antiangiogenic effect. Moreover, the mutant protein data point to the importance of eight residues surrounding and including the last cysteine as critical for endostatin activity. Given our present lack of knowledge of the protein conformation of the *E. coli*-generated proteins used in this study, it is not possible to conclude whether disulfide bonding (between cysteines 1 and 4 ; Ref. 40) is critical. Additional studies are in progress to address this issue.

At present, the origin of endostatin is not known. Collagen XVIII reported as a member of a family of collagen-like proteins is localized mainly in the perivascular portion of blood vessels (41, 42). Collagen XVIII by itself is not inhibitory to endothelial cells but when processed by as yet unknown mechanisms may lead to the release of the COOH-terminal portion (23). The proteases involved in the generation of endostatin is not clear, and how these may be regulated is also not known. The mechanism of endostatin-mediated tumor regression is unknown. Is there a receptor for endostatin on endothelial cells, and how does binding of endostatin to a putative endothelial cell-specific receptor initiate a cascade of events resulting in the inhibition of endothelial cell proliferation and migration? It is conceivable that endostatin may compete with binding of angiogenic stimulators such as bFGF and VEGF to its appropriate receptors? Alternatively, it is possible that proliferating endothelial cells up-regulate $\alpha_v\beta_3$, an endothelial integrin, and endostatin may act by disrupting the interaction of proliferating endothelial cells to matrix protein, thus driving endothelial cells to undergo apoptosis. It has been well documented that lack of attachment of endothelial cells to matrix protein may result in programmed cell death (43). Such mechanistic issues can now be addressed with our biologically active soluble version of yeast endostatin.

REFERENCES

1. Mulders, P., Figlin, R., deKernion, J. B., Wiltrout, R., Linehan, M., Parkinson, D., deWolf, W., and Belldegrun, A. Renal cell carcinoma: recent progress and future directions. Cancer Res., *57:* 5189–5195, 1997.

2. Maher, E. R., and Kaelin, W. G., Jr. von Hippel-Lindau disease. Medicine (Baltimore), *76:* 381–391, 1997.
3. Mukhopadhyay, D., Knebelmann, B., Cohen, H. T., Ananth, S., and Sukhatme, V. P. The von Hippel-Lindau tumor suppressor gene product interacts with Sp1 to repress vascular endothelial growth factor promoter activity. Mol. Cell. Biol., *17:* 5629–5639, 1997.
4. Gnarra, J. R., Zhou, S., Merrill, M. J., Wagner, J. R., Krumm, A., Papavassiliou, E., Oldfield, E. H., Klausner, R. D., and Linehan, W. M. Post-transcriptional regulation of vascular endothelial growth factor mRNA by the product of the VHL tumor suppressor gene. Proc. Natl. Acad. Sci. USA, *93:* 10589–10594, 1996.
5. Iliopoulos, O., Levy, A. P., Jiang, C., Kaelin, W. G. J., and Goldberg, M. A. Negative regulation of hypoxia-inducible genes by the von Hippel-Lindau protein. Proc. Natl. Acad. Sci. USA, *93:* 10595–10599, 1996.
6. Siemeister, G., Weindel, K., Mohrs, K., Barleon, B., Martiny-Baron, G., and Marme, D. Revision of deregulated expression of vascular endothelial growth factor in human renal carcinoma cells by von Hippel-Lindau tumor suppressor protein. Cancer Res., *56:* 2299–2301, 1996.
7. Iliopoulos, O., Kibel, A., Gray, S., and Kaelin, W. G., Jr. Tumour suppression by the human von Hippel-Lindau gene product. Nat. Med., *1:* 822–826, 1995.
8. Baillie, C. T., Winslet, M. C., and Bradley, N. J. Tumour vasculature–a potential therapeutic target. Br. J. Cancer, *72:* 257–267, 1995.
9. Bicknell, R. Vascular targeting and the inhibition of angiogenesis. Ann. Oncol., *5* (Suppl. 4)*:* 45–50, 1994.
10. Fan, T. P., Jaggar, R., and Bicknell, R. Controlling the vasculature: angiogenesis, anti-angiogenesis and vascular targeting of gene therapy. Trends Pharmacol. Sci., *16:* 57–66, 1995.
11. Thorpe, P. E., and Burrows, F. J. Antibody-directed targeting of the vasculature of solid tumors [see comments]. Breast Cancer Res. Treat., *36:* 237–251, 1995.
12. Burrows, F. J., and Thorpe, P. E. Vascular targeting–a new approach to the therapy of solid tumors. Pharmacol. Ther., *64:* 155–174, 1994.
13. Folkman, J. Tumor angiogenesis: therapeutic implications. N. Engl. J. Med., *285:* 1182–1186, 1971.
14. Folkman, J. Anti-angiogenesis: new concept for therapy of solid tumors. Ann. Surg., *175:* 409–416, 1972.
15. Folkman, J., and Shing, Y. Angiogenesis. J. Biol. Chem., *267:* 10931–10934, 1992.
16. Folkman, J. Fighting cancer by attacking its blood supply. Sci. Am., *275:* 150–154, 1996.
17. Maione, T. E., Gray, G. S., Petro, J., Hunt, A. J., Donner, A. L., Bauer, S. I., Carson, H. F., and Sharpe, R. J. Inhibition of angiogenesis by recombinant human platelet factor-4 and related peptides. Science (Washington DC), *247:* 77–79, 1990.
18. Gupta, S. K., Hassel, T., and Singh, J. P. A potent inhibitor of endothelial cell proliferation is generated by proteolytic cleavage of the chemokine platelet factor 4. Proc. Natl. Acad. Sci. USA, *92:* 7799–7803, 1995.
19. Angiolillo, A. L., Sgadari, C., Taub, D. D., Liao, F., Farber, J. M., Maheshwari, S., Kleinman, H. K., Reaman, G. H., and Tosato, G. Human interferon-inducible protein 10 is a potent inhibitor of angiogenesis *in vivo*. J. Exp. Med., *182:* 155–162, 1995.
20. Strieter, R. M., Kunkel, S. L., Arenberg, D. A., Burdick, M. D., and Polverini, P. J. Interferon gamma-inducible protein 10 (IP-10), a member of the C-X-C chemokine family, is an inhibitor of angiogenesis. Biochem. Biophys. Res. Commun., *210:* 51–57, 1995.
21. Brooks, P. C., Silletti, S., von Schalscha, T. L., Friedlander, M., and Cheresh, D. A. Disruption of angiogenesis by PEX, a noncatalytic metalloproteinase fragment with integrin binding activity. Cell, *92:* 391–400, 1998.
22. O'Reilly, M. S., Holmgren, L., Shing, Y., Chen, C., Rosenthal, R. A., Moses, M., Lane, W. S., Cao, Y., Sage, E. H., and Folkman, J. Angiostatin: a novel angiogenesis inhibitor that mediates the suppression of metastases by a Lewis lung carcinoma [see comments]. Cell, *79:* 315–328, 1994.
23. O'Reilly, M. S., Boehm, T., Shing, Y., Fukai, N., Vasios, G., Lane, W. S., Flynn, E., Birkhead, J. R., Olsen, B. R., and Folkman, J. Endostatin: an endogenous inhibitor of angiogenesis and tumor growth. Cell, *88:* 277–285, 1997.
24. Dong, Z., Kumar, R., Yang, X., and Fidler, I. J. Macrophage-derived metalloelastase is responsible for the generation of angiostatin in Lewis lung carcinoma. Cell, *88:* 801–810, 1997.
25. Lannutti, B. J., Gately, S. T., Quevedo, M. E., Soff, G. A., and Paller, A. S. Human angiostatin inhibits murine hemangioendothelioma tumor growth *in vivo*. Cancer Res., *57:* 5277–5280, 1997.
26. O'Reilly, M. S., Holmgren, L., Shing, Y., Chen, C., Rosenthal, R. A., Cao, Y., Moses, M., Lane, W. S., Sage, E. H., and Folkman, J. Angiostatin: a circulating endothelial cell inhibitor that suppresses angiogenesis and tumor growth. Cold Spring Harb. Symp. Quant. Biol., *59:* 471–482, 1994.
27. O'Reilly, M. S. Angiostatin: an endogenous inhibitor of angiogenesis and of tumor growth. Exper. Suppl. (Basel), *79:* 273–294, 1997.
28. Sim, B. K., O'Reilly, M. S., Liang, H., Fortier, A. H., He, W., Madsen, J. W., Lapcevich, R., and Nacy, C. A. A recombinant human angiostatin protein inhibits experimental primary and metastatic cancer. Cancer Res., *57:* 1329–1334, 1997.
29. Wu, Z., O'Reilly, M. S., Folkman, J., and Shing, Y. Suppression of tumor growth with recombinant murine angiostatin. Biochem. Biophys. Res. Commun., *236:* 651–654, 1997.
30. Standker, L., Schrader, M., Kanse, S. M., Jurgens, M., Forssmann, W. G., and Preissner, K. T. Isolation and characterization of the circulating form of human endostatin. FEBS Lett., *420:* 129–133, 1997.
31. Boehm, T., Folkman, J., Browder, T., and O'Reilly, M. S. Antiangiogenic therapy of experimental cancer does not induce acquired drug resistance [see comments]. Nature (Lond.), *390:* 404–407, 1997.
32. Kerbel, R. S. A cancer therapy resistant to resistance. Nature (Lond.), *390:* 335–336, 1997.
33. Eckart, M. R., and Bussineau, C. M. Quality and authenticity of heterologous proteins synthesized in yeast. Curr. Opin. Biotechnol., *7:* 525–530, 1996.
34. Cregg, J. M., Vedvick, T. S., and Raschke, W. C. Recent advances in the expression of foreign genes in *Pichia pastoris*. Biotechnology (NY), *8:* 905–910, 1993.
35. Dhanabal, M., Fryxell, D. K., and Ramakrishnan, S. A novel method to purify immunotoxins from free antibodies using modified recombinant toxins. J. Immunol. Methods, *182:* 165–175, 1995.
36. Iruela-Arispe, M. L., and Dvorak, H. F. Angiogenesis: a dynamic balance of stimulators and inhibitors. Thromb. Haemost., *78:* 672–677, 1997.
37. Fleer, R. Engineering yeast for high level expression. Curr. Opin. Biotechnol., *3:* 486–496, 1992.
38. Sudbery, P. E. The expression of recombinant proteins in yeasts. Curr. Opin. Biotechnol., *7:* 517–524, 1996.
39. Mauceri, H. J., Hanna, N. N., Beckett, M. A., Gorski, D. H., Staba, M-J., Stellato, K. A., Bigelow, K., Heimann, R., Gately, S., Dhanabal, M., Soff, G. A., Sukhatme, V. P., Kufe, D. W., and Weichselbaum, R. R. Interaction of angiostatin and ionizing radiation in anti-tumour therapy. Nature, *394:* 287–291, 1998.
40. Hohenester, E., Sasaki, T., Olsen, B. R., and Timpl, R. Crystal structure of the angiogenesis inhibitor endostatin at 1.5 Å resolution. EMBO J., *17:* 1656–1664, 1998.
41. Rehn, M., and Pihlajaniemi, T. Alpha 1(XVIII), a collagen chain with frequent interruptions in the collagenous sequence, a distinct tissue distribution, and homology with type XV collagen. Proc. Natl. Acad. Sci. USA, *91:* 4234–4238, 1994.
42. Muragaki, Y., Timmons, S., Griffith, C. M., Oh, S. P., Fadel, B., Quertermous, T., and Olsen, B. R. Mouse Col18a1 is expressed in a tissue-specific manner as three alternative variants and is localized in basement membrane zones. Proc. Natl. Acad. Sci. USA, *92:* 8763–8767, 1995.
43. Re, F., Zanetti, A., Sironi, M., Polentarutti, N., Lanfrancone, L., Dejana, E., and Colotta, F. Inhibition of anchorage-dependent cell spreading triggers apoptosis in cultured human endothelial cells. J. Cell Biol., *127:* 537–546, 1994.

Endostatin: Yeast Production, Mutants, and Antitumor Effect in Renal Cell Carcinoma

Mohanraj Dhanabal, Ramani Ramchandran, Ruediger Volk, et al.

Cancer Res 1999;59:189-197.